Scientific Report

Concerning the implementation of the project: January – December 2015

During the period covered by the present report, the research work carried out within the frame of the project entitled *Interactional and functional effects of the substrate on the electrochemical behavior of micro and nanostructured metallic and oxidic deposits* was directed towards two main objectives: the study of the effect of the surface structure of the pollycrystalline conductive diamond substrate on the electrochemical performances of supported electrocatalysts and the investigation of the possibility of using conductive diamond powder as support for such electrocatalyts. Results thus far clearly demonstrated that polycrystalline boron-doped diamond (BDD) is a material highly suited to be used as substrate for platinum-based electrocatalysts, in view of methanol fuel cell applications. Furthermore, it was observed that the modification of the BDD surface by replacing C–H bonds from the surface with oxygen-containing groups results in a significant enhancement of the resistance to CO poisoning during methanol oxidation of supported platinum (deposited as individual particles or being part of a Pt-oxide electrocatalytic material).

The particularly compact structure of polycrystalline diamond layers inherently leads to a rather low specific surface area of deposited electrocatalysts which limits to a certain extent possible practical applications of such systems. However, the possibility exists, at least in principle, to eliminate this drawback by using as substrate conductive BDD powder instead of a continuous conductive diamond film. This would obviously result in a significant increase of the specific area of the active material. It is widely known that the boron-doping level of the (111) crystallites from the polycrystalline diamond is *ca*. 10 times higher than that of the (100) ones which inherently leads to an inhomogeneity of the surface in terms of conductivity and, consequently, as Fig. 1 illustrates, to a nonuniform electrodeposition of platinum particles. Moreover, on the oxidized diamond (BDD-O) surface active sites at which $PtCl^{2-}$ takes places are partially blocked (as already mentioned in the previous report) by functional groups containing oxygen, thus favoring the formation of larger size clusters and the decrease of the specific active surface area of the electrocatalyst. The use of relatively large area films enables neglecting such effects because, usually, the two different types of crystallites are evenly distributed over the surface and the observed overall activity is in fact an average one. Conversely, when micrometric particles are used it is highly desirable that this inhomogeneity is somewhat mitigated in order to have a distribution of the deposited particles as uniform as possible.

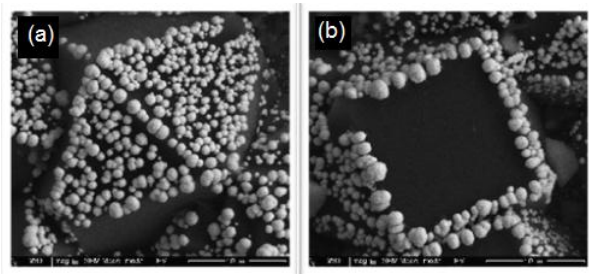

Fig. 1 SEM micrographs of platinum electrodeposited on (111) (a) and (100) (b) crystallites from the polycrystalline BDD surface.

Previous results indicate that such mitigation could be achieved by modifying the surface of the BDD with various amounts of deposited semiconducting oxides.

Based upon the above considerations, at this stage of the research the influence of the surface oxygen-containing groups on the electrochemical deposition of stable oxides was investigated, together with the possibility of obtaining BDD-O supported Pt-oxide composites with suitable electrocatalytic features. Starting from previous results, attention was given to titanium oxide but preliminary studies were also carried out in order to assess the possibility of using also electrodeposited hydrous ruthenium oxide ($RuO_x \cdot nH_2O$). This was because data from the literature seem to prove that ruthenium oxide itself is a good electrocatalyst for carbon monoxide oxidation at room temperature, its presence being susceptible to contribute to a better desorption of CO species from the active sites of platinum, thus enabling better resistance to fouling of the electrocatalyst.

Electrochemical, surfactant-mediated, deposition of hydrated titanium oxide was accomplished by a straightforward method, previously described in detail. Concisely, a TiO_2 amorphous film was anodically deposited on the BDD electrodes from a 0.1 M KCl + 50 mM $TiCl_3$ solution (pH, 2.2), in the presence of a concentration of 0.25 mM sodium dodecyl sulfate (SDS). The deposition potential was 0.85 V and the titanium oxide loading was controlled by appropriately adjusting the deposition time. Prior to titanium oxide deposition, BDD samples were subjected either to a cathodic hydrogenation treatment or to an anodic oxidation one, in order to achieve hydrogen-terminated (BDD-H) or oxygen-terminated surfaces. Cathodic and anodic pre-treatments were carried out (according to slightly modified versions of methods described in the literature) for 30 min. in a 0.1 M $HClO_4$ aqueous solution, at an applied potential of -2.5 and 3.0 V, respectively.

In order to appraise the extent to which SDS interferes in the overall charge transfer processes occurring at the BDD surface, cyclic voltammetry in a 0.1 M KCl + 1 mM $K_4Fe(CN)_6$ solution was firstly used and Fig. 2 shows typical results obtained at BDD-H and BDD-O, both in the absence (curves 1) and in the presence (0.25 mM) of SDS (curves 2). At hydrogen-terminated diamond electrodes the shape of the voltammetric response recorded for $K_4Fe(CN)_6$ dramatically changes upon SDS addition. Thus, as curve 2 from Fig. 2a illustrates, in the presence of the surfactant the peak for the oxidation of $[Fe(CN)_6]^{4-}$ ions shifts towards higher potential which clearly indicates a significant decrease in the heterogeneous electron transfer rate constant. We can conjecture that an adsorption layer is formed on the

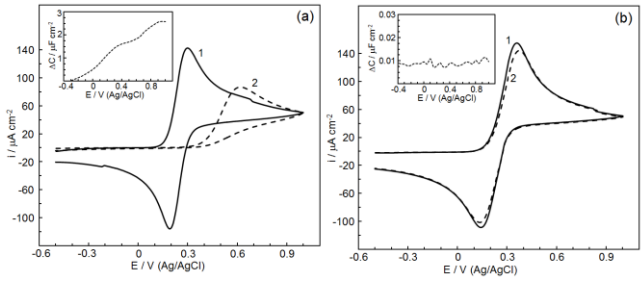

Fig. 2 Voltammograms in 0.1 M KCl + 1 mM $K_4Fe(CN)_6$ (50 mV s^{-1}) for BDD-H (a) and BDD-O (b) in the absence (1) and in the presence of 0.25 mM SDS (2). Insets: potential dependence of the difference between the capacitance in the presence and in the absence of SDS.

electrode, because of the strong interaction between the hydrophobic hydrogen-terminated BDD surface and the alkyl chain of the SDS. Differential capacitance measurements were also carried out at BDD-H and BDD-O electrodes in a 0.1 M KCl solution (in the absence of redox species) both before and after SDS addition. SDS accumulation at the electrode surface was gauged by means of the difference (ΔC) between the capacitance in the presence of the surfactant and that in its absence, and the effect of the applied potential on this process is illustrated in the insets from Fig. 2. At BDD-H electrodes SDS adsorption is perceptible starting from *ca*. -0.4 V and becomes more important at higher potentials, the increase of ΔC reaching a pseudo-plateau at an applied potential of *ca*. 0.3 V. This value roughly corresponds to the onset potential of the ferrocyanide oxidation current (see curve 2 in Fig. 2a), indicating that, in the presence of SDS, $[Fe(CN)_6]^{4-}$ oxidation takes place on the partially blocked BDD-H surface. As Fig. 2b shows, at BDD-O, the presence of the surfactant did not affect significantly the voltammetric response recorded with $K_4Fe(CN)_6$. This is because the hydrophilic surface of the oxygen-terminated BDD would foreclose SDS adsorption by dint of attraction between the electrode and the hydrophobic tail of surfactant molecules. Indeed, as the inset from Fig. 2b illustrates, the increase of the capacitance induced by the addition of the surfactant is with *ca*. two orders of magnitude lower than that observed at BDD-H and, within the investigated potential range, ΔC is basically not affected by the variation of the applied potential.

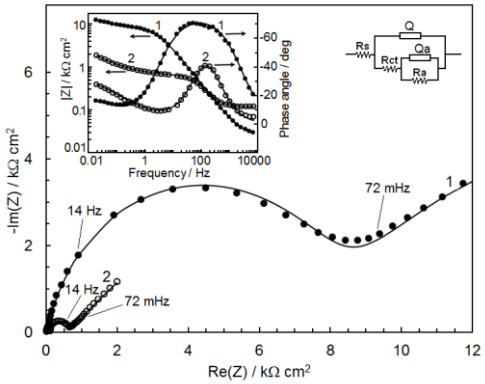

Fig. 3 EIS results at BDD-H (1) and BDD-O (2), in 0.1 M KCl + 1 mM $K_4Fe(CN)_6$ + 0.25 mM SDS, at an applied potential of 0.50 and 0.25 V, respectively. Insets: corresponding Bode representations and associated equivalent circuit. Solid lines show the result of the simulation.

EIS measurements were also performed in a 0.1 M KCl + 1 mM $K_4Fe(CN)_6$ + 0.25 mM SDS solution and the applied potential was that corresponding to the values of the half-peak potential evidenced by cyclic voltammetry (0.50 V and 0.25 V for BDD-H and BDD-O electrodes, respectively). As these results suggests (see the shape of the Bode plots from the inset in Fig. 3), in the investigated frequency range, the impedance response could be simulated by an equivalent circuit with two time constants, akin to those usually associated to electrode processes that involve adsorption/desorption equilibria. This equivalent circuit (inset in Fig. 3) includes the resistance of the solution (Rs), the charge transfer resistance (Rct) and the resistance imposed by the SDS adsorption at BDD electrodes (Ra). Due to the inherent roughness of the surface and to its physical inhomogeneity, the capacitance of the double layer and the adsorption pseudocapacitance were simulated by means of constant phase elements (Q and Qa, respectively). The very good agreement between experimental and calculated EIS data (chi-square lower than 10^{-3}) allowed trustworthy estimation of the equivalent circuit parameters among which the charge

transfer resistance is of particular interest. Thus, values of Rct of 8.3 kΩ cm^2 and 0.5 kΩ cm^2 were calculated for BDD-H and BDD-O respectively, in line with the EIS behavior illustrated by the Nyquist representations from Fig. 3. These are further evidence of the fact that the presence of sodium dodecyl sulfate strongly hinders redox processes occurring at the hydrogen-terminated BDD surface, while the oxidized one is free of such problems, in concurrence with the results of cyclic voltammetry experiments.

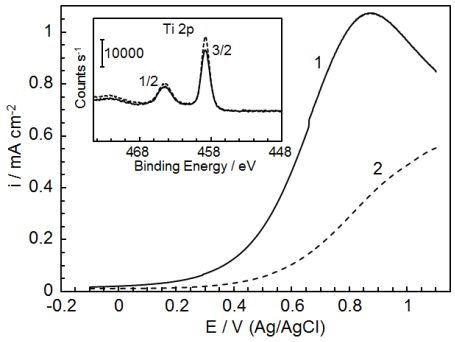

Fig. 4 Linear sweep voltammograms (sweep rate, 10 mV s^{-1}) recorded at BDD-O (1) and BDD-H (2) electrodes in a 0.1 M KCl + 50 mM $TiCl_3$ solution (pH, 2.2) in the presence of SDS (0.25 mM). Inset: narrow-scan XPS spectra in the Ti 2p region for titanium oxide deposited on BDD-O (dashed line) and BDD-H (solid line); deposition charge, 320 mC cm^{-2}.

The part that the chemical termination of the BDD surface plays in the surfactant-mediated anodic deposition of titanium dioxide was firstly scrutinized by linear sweep voltammetry (sweep rate, 10 mV s^{-1}) and Fig. 4 shows characteristic responses obtained in the presence of SDS for Ti(III) oxidation, both at BDD-O and BDD-H. It was found that at hydrogen-terminated BDD electrodes anodic formation of titanium oxide is a slow (kinetically controlled) process, as indicated by the shape of curve 2 from Fig. 4. Conversely, at oxygen-terminated BDD, Ti(III) oxidation is affected to a much lesser extent by surfactant addition and the shape of the voltammetric response (curve 1 from Fig. 4) is typical for a process under both kinetic and diffusional control. This is why at the value of the potential applied for TiO_2 surfactant-assisted deposition (0.85 V) the anodic current density is lower at BDD-H electrodes (compare curves 1 and 2 from Fig. 4). Therefore, in order to assess the effect of the surface termination, only electrodes with titanium oxide loadings obtained by using similar deposition charges (320 ± 2% mC cm^{-2}) were further compared on a relative basis. The inset in Fig. 4 shows typical XPS spectra in the Ti 2p region recorded for two such electrodes, with BDD-O (solid line) and BDD-H (dashed line) substrates. The value of the binding energy corresponding to the $2p_{3/2}$ peak (458.8 eV) as well as the clear similarity between the narrow-scan spectra demonstrates titanium oxide formation on both diamond supports.

Fig. 5 shows characteristic SEM micrographs obtained for titanium oxide coatings deposited under the same experimental conditions , both on BDD-O (Fig. 5a) and BDD-H (Fig. 5b) substrates. It can be observed that, at the oxidized BDD surface, there is tendency for the electrodeposited oxide to accumulate at the boundaries between diamond crystallites and at their edges, probably due to a higher current density in these zones. On the contrary, with hydrogen-terminated BDD as support, the coatings are obviously more uniform and small size (30 to 150 nm) oxide clusters are homogeneously distributed over the entire surface of the electrodes. This would lead to a higher roughness of the surface, with possible beneficial effects in terms of electrochemically active area. It appears that, in the

case of the BDD-H substrate, the presence of the stable SDS adsorption layer can assist in mitigating this inhomogeneity of the electrode surface in terms of conductivity, resulting in a more uniform titanium oxide coating. The photoelectrochemical activity of titanium oxide coatings formed by SDS-mediated anodic deposition (both on BDD-O and BDD-H substrates) was gauged in a potentiodynamic regime (sweep rate, 10 mV s^{-1}), under intermittent UV irradiation, and typical responses for electrodes with similar oxide loadings are shown in the insets from Fig. 5. A higher dark current was observed for TiO_2 supported on hydrogen-terminated BDD, presumably due to a higher electrochemically active surface area, in line with the somewhat rougher structure of the coatings evidenced by SEM. Nevertheless, it appeared that, in terms of possible photoelectrochemical applications, hydrogen-terminated BDD is better suited to be used as substrate for titanium oxide. Thus, it was observed that, at an applied potential of 0.85 V, titanium oxide deposition on BDD-H allows obtaining an increase of *ca*. 2.5 times of the current under irradiation, compared to the case in which BDD-O was used as support (see insets in Fig. 5b and 5a, respectively). On the other hand, in the first case the dark current was found to be only *ca*. 1.9 times higher, most likely due to a corresponding enhancement of the oxide deposit surface area. These findings suggest that the improvement of the photoresponse enabled by the BDD-H substrate can not be ascribed exclusively to an increase of the electrochemically active surface area. Thus, there are reasons to believe that the smaller size of the TiO_2 clusters, as well as their more homogeneous distribution on the hydrogen-terminated BDD surface, could contribute to some extent to a less important bulk recombination of charge carriers, with beneficial effects on the photoelectrochemical activity.

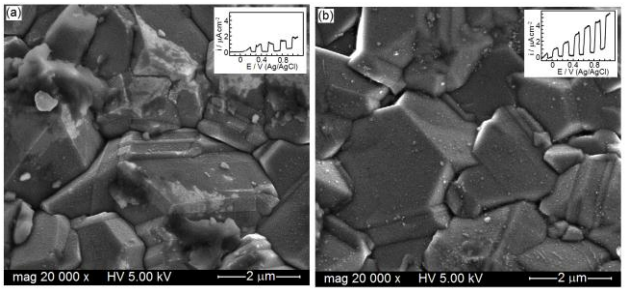

Fig. 5 SEM micrographs for titanium oxide deposited on BDD-O (a) and BDD-H (b) electrodes. Deposition charge (mC cm^{-2}): (a) 325; (b) 321. Insets: corresponding current-potential dependence upon intermittent UV irradiation.

Hydrous ruthenium oxide was deposited from an aqueous solution containing 5 mM $RuCl_3 \cdot nH_2O$, 0.1 M KCl and 0.01 M HCl, by continuously cycling the potential of the electrode within the range -0.2 to 1.0 V at scan rate of 20 mV s^{-1}. In the second step, platinum deposition was achieved from a 0.1 M $HClO_4$ + 2.4 mM H_2PtCl_6 solution, by applying consecutive potentiostatic pulses (applied potential, -0.1 V) of two seconds' each, and the cathodic charge integrated during this process was used for calculating the corresponding Pt loading. In order to assess $RuO_x \cdot nH_2O$ formation on the BDD surface, the pseudocapacitance of oxide-modified electrodes was investigated by cyclic voltammetry within the potential range -0.2 to 1.0 V, at a sweep rate of 50 mV s^{-1}, in 0.1 M $HClO_4$ solution. Fig. 6 shows voltammetric responses, typical of the behavior of hydrous ruthenium oxide in acidic media, recorded after six consecutive deposition cycles, performed both with BDD-H and BDD-O

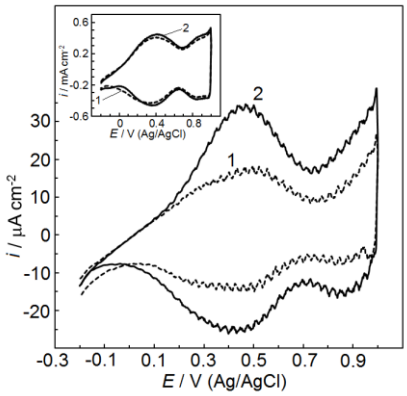

Fig. 6 Voltammograms after six consecutive $RuO_x \cdot nH_2O$ deposition cycles at BDD-H (1) and BDD-O (2). Inset: responses at the same electrodes after 60 deposition cycles. Electrolyte, 0.1 M $HClO_4$; sweep rate, 50 mV s^{-1}.

electrodes (curves 1 and 2, respectively). The voltammetric charge integrated (as the average of the anodic and cathodic charges) within the potential range 0.0 to 1.0 V can be used as a measure of the amount of deposited $RuO_x \cdot nH_2O$ and, by taking into account a value of 121.5 C g^{-1} reported for BDD-supported hydrous ruthenium oxide, loadings of *ca*. 1.7 μg cm^{-2} and *ca*. 3.1 μg cm^{-2} were estimated for $RuO_x \cdot nH_2O$/BDD-H and $RuO_x \cdot nH_2O$/BDD-O, respectively. It therefore appears that the use of oxidized BDD as substrate enables more efficient ruthenium oxide formation. As the inset in Fig. 6 shows, after 60 consecutive cycles the effect of the substrate is less marked and similar amounts of $RuO_x \cdot nH_2O$ were deposited both on BDD-H and BDD-O (*ca*. 133 and *ca*. 140 μg cm^{-2}, respectively, as estimated from the corresponding voltammetric charges). To appraise the influence of the hydrous ruthenium oxide substrate on the electrocatalytic performances of deposited platinum, the activity for methanol oxidation of the Pt–$RuO_x \cdot nH_2O$/BDD-O electrodes was firstly checked by cyclic voltammetry and Fig. 7 shows typical responses. Electrodes obtained by electrochemical deposition of Pt on bare BDD-O were also used for comparison. At Pt–$RuO_x \cdot nH_2O$/BDD-O with low oxide loading (curve 2 from Fig. 7), the potential of the forward anodic peak exhibits a shift of *ca*. 80 mV toward lower values, indicating that, compared to the case of Pt/BDD-O, the overall process is facilitated to some extent, due to a slight, but nonetheless significant co-catalytic effect of the hydrous ruthenium oxide substrate. As curve 3 from Fig. 7 shows, an increase of the $RuO_x \cdot nH_2O$ loading, up to *ca*. 140 μg cm^{-2}, strongly promotes methanol oxidation, as proved by the much more substantial cathodic shift of the main oxidation peak. Further experiments are in progress in order to explain this behavior. The above results were partially published in the following papers:

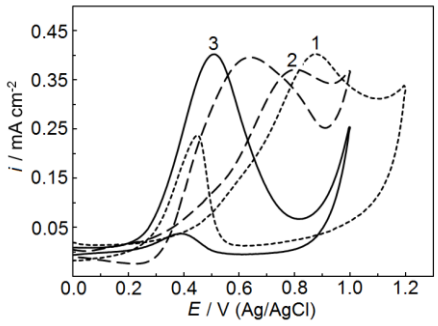

Fig. 7 Cyclic voltammograms recorded in a 0.1 M $HClO_4$ + 3.22 M CH_3OH solution (20 mV s^{-1}) for Pt/BDD-O (1) and Pt–$RuO_x \cdot nH_2O$/BDD-O (2, 3) electrodes. Platinum loading, 5 μg cm^{-2}; oxide loading (μg cm^{-2}): (1) 0, (2) 3, (3) 140.

- „Influence of boron-doped diamond surface termination on the characteristics of titanium dioxide anodically deposited in the presence of a surfactant" published in *Journal of The Electrochemical Society* **162** (2015) H535–H540.

- „Electrochemical deposition of Pt-RuOx·nH_2O composites on conductive diamond and its application to methanol oxidation in acidic media" – *Electrocatalysis*, Accepted for publication, DOI: 10.1007/s12678-015-0292-8.